Reaction Kinetics at Dispersed-Colloid/Solution Interfaces: Benzophenone Triplet-State Quenching by Methylated Silica Particles

Stephanie R. Shield and Joel M. Harris*

Department of Chemistry, University of Utah, 315 South 1400 East, Salt Lake City, Utah 84112-0850

Received: April 17, 2000; In Final Form: July 12, 2000

Dispersed silica colloids are used as model surfaces for studying triplet-state reaction kinetics at liquid/solid interfaces. Phosphorescence from the triplet state of benzophenone is quenched by a hydrogen-atom abstraction from methyl groups immobilized on the surface of a silica colloid. The production of diphenylketyl radicals from this Norrish Type II reaction and their decay by recombination are also monitored using a time-resolved laser-induced fluorescence technique. Aggregation of the colloids results in a dispersion of benzophenone-triplet quenching rates; the fractions of excited-triplet states quenched by small clusters and larger aggregates were estimated and used to determine rate constants for reaction with the two populations of surface methyl groups. The rates of the interfacial reactions of triplet benzophenone were enhanced compared to reactions in free solution, which is likely due to weak adsorption of triplet benzophenone to the methylated silica surface.

Introduction

The photophysics and photochemistry of molecules at liquid/solid interfaces are important in many areas of science including environmental photochemistry,[1] heterogeneous photocatalysis,[2,3] and photobinding and photocuring processes used to modify the interfacial properties of materials.[4−10] Monitoring the fate of electronically excited states and photolytically generated radicals that may participate in subsequent reactions at the interface is an important goal in controlling and understanding these processes. Photophysical methods are also useful in measuring interfacial transport kinetics and reaction mechanisms, using a laser pulse to initiate a reaction and time-resolved spectroscopy to monitor the decay of the excited population at the surface.[11−20]

Flat surfaces have traditionally been used as substrates for studies of interfacial reactions from the gas phase; they are compatible with high vacuum surface-science techniques to determine the extent of reaction and the structure and properties of the surface monolayers. Flat surfaces are rarely used in studies of photoreactions at liquid/solid interfaces due to their low surface area and correspondingly small number of molecules at the interface compared with the large population of molecules in the overlying liquid solution. To overcome this limitation, most studies of photophysics and photochemistry at liquid/solid interfaces have been carried out using porous solids such as silica gel. Silica gel has a very high specific surface area, is optically transparent in the near-UV and visible regions, and can be easily surface-derivatized,[21] making it convenient for studying photoinitiated reaction kinetics at interfaces.[11−15] Fluorescent probes have been adsorbed or covalently bound onto porous silica in order to study rates of excited-state quenching at the liquid/solid interface.[16−20] Short-range transport in silica on a nanosecond time scale has been found to be efficient, comparable to diffusion rates in free solution.[22] Longer-range diffusion may be slower, hindered by the influence of the pore network,[23−25] which can complicate the interpretation of slower reaction kinetics in porous silica materials.

To improve transport efficiency over longer distances while preserving the high specific surface area typical of porous silica, we propose using nonporous, fumed silica particles dispersed in solution to investigate kinetics of interfacial photoinitiated reactions. Colloidal particles dispersed at modest concentrations can provide a high concentration of surface sites for reaction. For example, a 1% suspension (10 mg/mL) of a typical fumed silica having a specific surface area of 250 m^2/g and a modest reactive surface site coverage of 5 $\mu mol/m^2$ can provide a high concentration (12.5 mM) of reactive groups in a dispersed sample. The nature of photochemical kinetics on colloids is important in understanding environmental photochemistry on dispersed solid surfaces. While fumed silica has been used as an adsorbent support for studying photophysics at gas/solid interfaces,[26−30] few studies of photophysics at solution/dispersed-particle interfaces have appeared in the literature. One such study of fluorescence quenching of a pyrene probe immobilized to a fumed silica surface[31] showed that well-dispersed colloids allow efficient molecular transport from solution and interfacial encounter kinetics that approach free-solution diffusion-controlled rate limits.

In this work, we employ fumed-silica colloids as a model surface for investigating interfacial photochemical reaction kinetics, in particular, H-atom abstraction from a surface-immobilized donor group by triplet benzophenone. While the photochemistry of immobilized excited singlet[16−20] and excited-triplet[32] probes has been used to investigate reaction kinetics at liquid/solid interfaces, interfacial kinetics involving a free-solution excited state and a chemically bound quencher have not been widely studied. In our experiment, a methylated fumed-silica colloid acts as an immobilized quencher of the free-solution benzophenone triplet state, which was monitored by its phosphorescence emission. The excited-state decay kinetics are compared to homogeneous free-solution quenching of the triplet state by methanol and hexamethyldisiloxane, and the rate constant for H-atom abstraction from methyl groups bound to the colloid surface by triplet benzophenone is determined. To check the mechanism of quenching and yield of free radicals, the diphenylketyl radical was detected using time-resolved fluorescence,[33] and rates of ketyl-radical recombination were measured.

10.1021/jp0014420 CCC: $19.00
Published on Web 08/12/2000

Experimental Section

Instrumentation. A frequency-tripled Quanta Ray model GCR-11 Nd:YAG laser ($\lambda_e = 355$ nm) was operated at 10 Hz and intermittently blocked by a shutter to provide a repetition rate of 1.0 Hz. The 5 ns UV (90 μJ) excitation pulse was weakly focused to a spot size of 2.2 mm and used to photoexcite the sample. Fluorescence of transient diphenylketyl radicals was excited by a Lexel model 95 continuous wave argon-ion laser ($\lambda_p = 514.5$ nm) which was focused to a spot size of 380 μm in the sample at a power of 500 mW.

Fluorescence and phosphorescence were collected at 90° from the excitation axis and filtered through a 1.0 cm path of a 5% aqueous solution of sodium nitrite and three glass filters (Schott KV408, KV550, and OG570). The filtered emission was detected by a Hamamatsu R976 photomultiplier tube and digitized with a LeCroy 9450 oscilloscope. Fifty phosphorescence transients or 200 fluorescence transients were averaged. An oscilloscope input termination resistance of 50 Ω was used for collection of the phosphorescence decay data with 10 ns resolution, while a resistance of 1 MΩ was used to monitor fluorescence from the ketyl radical with an *RC*−time constant of 100 μs.

Reagents. The hydrophobic, methylated fumed silica (Aerosil R976) was used as received from the Degussa Corp. This nonporous silica is produced by flame oxidation and then modified with dimethyldichlorosilane in the gas phase to produce the hydrophobic silica material. The particles have a mean particle diameter of 7 nm and a specific surface area of 250 m^2/g.[34] The weight percent carbon content of the methylated colloids was determined to be 1.44% by elemental analysis at M−H−W Laboratories (P.O. Box 15853, Phoenix, AZ 85060). Using the carbon weight percent and the colloid surface area, the surface coverage of methyl groups is estimated to be 4.8 μmol/m^2. Unreacted silanols on the surface are reported at a concentration of 0.8 μmol/m^2,[34] or approximately 15% of the methyl surface coverage.

Benzophenone (BP) 99% from Aldrich, benzhydrol (BPH_2) 99% from Aldrich, acetonitrile (ACN) glass distilled from OmniSolve, methanol (MeOH) spectrograde from Optima, and hexamethyldisiloxane (HMDS) 99.5% from Aldrich were used without further purification. Sodium phosphate monobasic (Mallinckrodt, AR) and sodium phosphate dibasic heptahydrate (Mallinckrodt, AR) were heated to 120 °C for 2 h, cooled in a desiccator, and used to prepare a buffer for the solutions. Water was purified with a Corning still (MP-1) and a Barnstead Nanopure four-cartridge purification system, was passed through a 0.2 μm filter, and exhibited an electrical resistivity of 18 MΩ•cm A phosphate buffer solution of pH = 6.4 (80 mM $H_2PO_4^-$ and 5.5 mM HPO_4^{2-}) was used to reduce colloidal aggregation. The pH values were not corrected for changes in the reference-electrode liquid-junction potential in mixed solvents; these corrections to pH, however, are small (0.15 pH units) and constant for a given mixed solvent composition.[35,36]

Procedures. The colloid suspensions were mechanically stirred overnight in order to disperse the silica; the suspensions were continuously stirred throughout the experiment to prevent any settling. Oxygen was removed from benzophenone-containing solutions via four freeze−pump−thaw cycles pumped to a base pressure of ≤50 μTorr. Under these conditions, a 100 μM solution of BP produced an unquenched triplet lifetime of ≈150 μs in a 50/50 (v/v) acetonitrile/water solution. To reduce the buildup of photoproducts in the excitation region of the sample, the solution was magnetically stirred during data acquisition. In addition, a large volume (10 mL) of solution was transferred into the 1 cm path length quartz freeze−pump−thaw cell, and the sample was shaken between collection of each set of transients.

A negative offset in the baseline was observed in the ketyl radical fluorescence transients in 50/50 ACN/H_2O at pH = 7.1 (30 mM $H_2PO_4^-$ and 30 mM HPO_4^{2-}) after UV excitation. The direction of the offset was indicative of UV photobleaching of a fluorescent impurity that was excited at 514 nm. Consistent with this behavior, after about 150 pulses (≈14 mJ) of UV excitation, the negative baseline disappeared and fluorescence from the ketyl radical could be observed free of offset. At pH = 7.1, the negative baseline was 27% of the radical fluorescence signal amplitude; it was reduced to below the noise level following UV photolysis while the radical fluorescence signal was unaffected. At a lower pH = 6.4, the initial negative baseline was only 9% of the signal amplitude and was reduced to below the noise level after approximately 100 UV laser shots. Experiments were performed at pH = 6.4 (phosphate buffer) and samples were exposed to approximately 100 UV shots before acquiring fluorescence data.

Infrared absorption data on the methylated silica were acquired as a thin-film transmission spectrum using a Bruker IFS 66v FTIR spectrometer. The silica was deposited onto both sides of a germanium window by dip coating (40 dips at a withdrawal rate of 1.0 cm/s) from a 1% (w/v) suspension of the particles in 2-propanol. The resulting films were dried in a 200 °C oven for 1 h to remove solvent, and infrared spectra were acquired under vacuum. As a check for either physisorbed or chemisorbed 2-propanol influencing the results, a comparable underivatized fumed silica (Aerosil 200, Degussa) film was deposited and processed in the same manner; no infrared absorption in the C−H stretching region could be detected from this control sample.

Scanning electron microscopy (SEM) images of the colloidal dispersions were acquired using a Cambridge Instruments Stereoscan 240. Samples were prepared in the same manner as for the quenching studies including the freeze−pump−thaw process. Prior to deposition on an aluminum SEM substrate, the solutions were diluted 100-fold to avoid further aggregation of the particles during solvent evaporation. Dilutions were performed quickly, and 4 μL aliquots of the diluted suspensions were immediately deposited onto an aluminum substrate. The sample droplet was spread out over an area of approximately 1 cm^2 by sandwiching the drop between a second aluminum substrate; the top substrate was then removed, and the solvent was allowed to evaporate in a desiccator before overcoating with gold for SEM imaging.

Data Analysis. Phosphorescence transients were collected at a laser pulse energy of 90 μJ/pulse for colloid concentrations of 0, 2.7, 6.2, 10.6, and 15.1 mg/mL, which correspond to methyl-group concentrations of 0, 3.2, 7.4, 12.7, and 18.1 mM. The rate constant for the quenching of triplet benzophenone by the methylated fumed silica particles was determined from changes in the benzophenone phosphorescence decay rate. The colloid reaction kinetics were compared to free-solution quenching kinetics by methanol and hexamethyldisiloxane. A laser pulse energy of 370 μJ/pulse was used for methanol concentrations varying from 0 to 35 mM and a laser pulse energy of 150 μJ/pulse was used for hexamethyldisiloxane concentrations ranging from 0 to 30 mM in order to determine the rate constants for free-solution quenching by these compounds.

Fluorescence from the excited doublet state of the diphenylketyl radical intermediate was observed over a 200 ms time window and fit to a second-order decay model. Subtraction of

the probe-only and pump-only transients was necessary to resolve the ketyl radical fluorescence from triplet-benzophenone phosphorescence and background fluorescence.[33] Photoexcited ketyl radical fluorescence was collected at the lowest colloid concentration, 2.7 mg/mL, to avoid excessive laser scattering.

All time-resolved transients were fit to their respective kinetic models using a program compiled in Microsoft Fortran, where a Marquardt algorithm was employed to optimize the kinetic parameters and signal amplitudes. Uncertainties in rate constants and plotted error bars are reported as ±1 standard deviation.

Results and Discussion

To investigate the reaction kinetics of excited-triplet states at colloidal-solid/liquid interfaces, we measured the rates of quenching of excited-triplet states of benzophenone by methyl groups bound to fumed silica particles that are dispersed in solution. The triplet state of benzophenone is produced in step 1a by photoexcitation of the ground state to the excited singlet state and subsequent efficient intersystem crossing to the triplet manifold.

$$Ph_2CO \xrightarrow{h\nu} {}^1Ph_2CO \rightarrow {}^3Ph_2CO \qquad (1a)$$

Phosphorescence and nonradiative decay of the excited-triplet state occur in step 1b.

$${}^3Ph_2CO \xrightarrow{k_o} Ph_2CO \qquad (1b)$$

The proposed mechanism for the quenching of triplet benzophenone by methyl groups chemically bound to fumed silica is via H-atom abstraction,[37−44] producing a diphenylketyl radical and a silica-bound methylene radical.

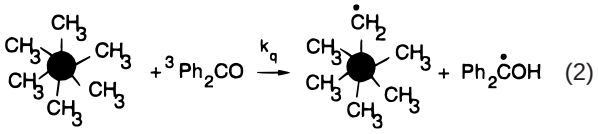

(2)

The solid core of the colloid represents the SiO_2 network in the particle. Unreacted silanols are present at about 15% of the methyl concentration (0.8 μmol/m^2).[34] On the basis of a quenching study with nonderivatized silica colloids (see below), the bare silica surface does not quench triplet benzophenone within the reproducibility of the kinetic measurements.

Determination of the Quenching Rate Constant. The quenching kinetics of the triplet state of benzophenone by methylated fumed silica were determined from changes in the decay rate of benzophenone phosphorescence. The concentration of methyl groups was varied by changing the amount of suspended colloid, and the quenching rate constant was evaluated by a Stern−Volmer analysis. Phosphorescence from the unquenched benzophenone samples fit a single first-order decay model. As methylated-silica colloids were added, however, the phosphorescence decay becomes biexponential, indicating the presence of two distinguishable populations of excited states that are not averaged during the excited-state lifetime. Figure 1 shows example phosphorescence transients together with the best fit biexponential decay for the total methyl-group concentration [$-CH_3$] ranging from 3.2 to 18.1 mM.

Several possibilities exist for the presence of different excited-state populations when colloids are added to the sample: some fraction of benzophenone could be adsorbed to the colloid surface, the surface chemistry of the colloids could be inhomogeneous, or a dispersion in colloid aggregation could be affecting

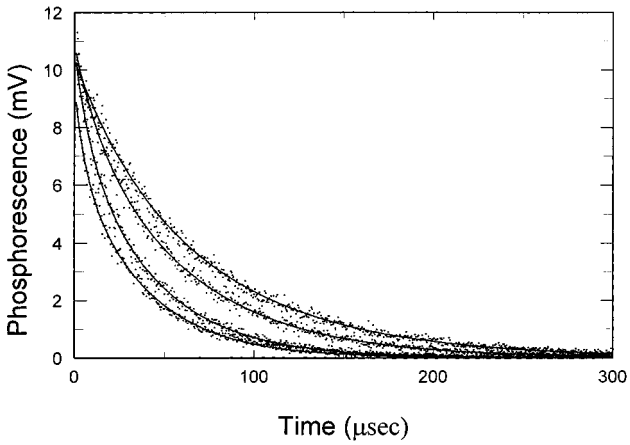

Figure 1. Phosphorescence emission from triplet benzophenone quenched by methylated colloids. Experiments were done in 50/50 ACN/H_2O at pH = 6.2 with dispersed methyl-group concentrations of 3.2, 7.4, 12.7, and 18.1 mM. The smooth curves are best fits to the sum of two exponential decays.

the rates of quenching. Chromatographic retention of benzophenone on a methylated silica (C1) column was measured using a 50/50 ACN/H_2O mobile phase to determine the fraction of adsorbed benzophenone. From the retention time (t_0) of an unretained species (D_2O) and the retention time of benzophenone (t_r), a capacity factor, $k' = (t_r - t_0)/t_0$, can be calculated, which represents the fraction of adsorbed benzophenone on the methylated silica surface. A significant increase in the retention of benzophenone compared to D_2O was not detectable by this method; on the basis of retention time uncertainty, however, an upper bound can be placed on the capacity factor of benzophenone, $k' \leq 0.02$. The rate of adsorption of uncharged solutes to methylated silica has been measured by temperature-jump relaxation and was found to occur at a diffusion-controlled rate;[45] this result, together with the upper bound for the capacity factor and the methyl-group surface-site density can be used to estimate a lower bound to the desorption rate, $k_{des} \geq 1.6 \times 10^6$ s^{-1} or an upper bound for the residence time on the surface, $\tau_{res} = 1/k_{des} \leq 600$ ns. Since the surface residence time is much shorter than the lifetime of the triplet state, any adsorption contributions to heterogeneity would be *averaged* during the excited-state lifetime and, therefore, cannot lead to a dispersion in decay rates.

To characterize dispersion in the silica surface chemistry, an infrared study was performed by dip-coating a thin film of the methylated colloids onto a germanium window to acquire a spectrum of the hydrocarbon species on the surface. The results, shown in Figure 2, indicate that the surface contains only (>95%) methyl groups. Triplet quenching by the bare silica surface was tested by using Aerosil 200 (Degussa), the underivatized fumed silica of similar particle size. The benzophenone triplet lifetime was unaffected by additions of bare silica sol that produce silanol concentrations corresponding to those found in the methylated-colloid quenching studies. For a series of bare silica suspensions producing 0−1.0 mM SiOH in solution, the observed benzophenone triplet lifetime varied randomly about an average of 140 μs (standard deviation = 12 μs) with a quenching rate constant that was indistinguishable from zero. For methylated colloid suspensions ([$-CH_3$] = 0−5.7 mM) having equivalent silanol concentrations, however, the benzophenone triplet lifetime decreased systematically to a value of 80 μs at the highest colloid concentration. On the basis of these results, it is clear that quenching is dominated by the methyl groups on the colloid and that quenching by residual

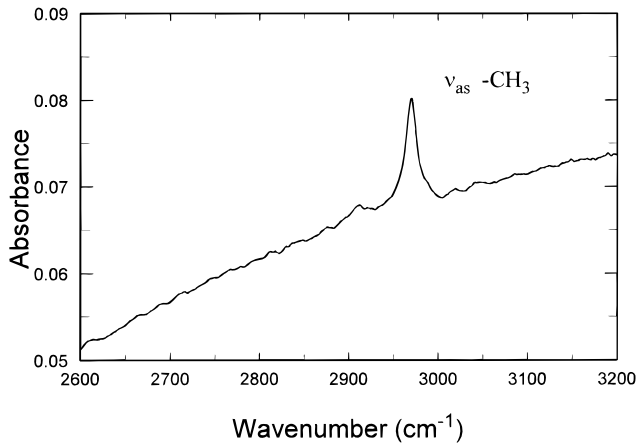

Figure 2. FTIR spectrum of a film of methylated colloids deposited onto a germanium window. The strong peak at 2970 cm^{-1} is indicative of the asymmetric C−H stretch for methyl groups. The weak peak at 2910 cm^{-1} could be an asymmetric stretch of methylenes, but the peak area is only 5% of that of the methyl C−H stretch.

silanols is negligible. From all of these results, we conclude that inhomogeneous triplet decay in the presence of methylated colloids cannot be explained by a dispersion in hydrocarbon structure, differences in the decay of adsorbed species, or quenching by surface silanols.

A dispersion in colloidal aggregation could account for differences in benzophenone triplet decay rates. Two classes of colloid aggregates can be detected in SEM images (see Figure 3). At low concentrations, the colloids are present as small clusters (Figure 3a). As the concentration of colloids increases, a higher fraction of particles exist as large aggregates (Figure 3b,c); Figure 3d shows the SEM image of methylated colloids at high concentrations with micrometer-sized aggregates. Within these aggregates, benzophenone would be exposed to a locally higher concentration of methyl groups while dispersed, smaller clusters would produce a lower local concentration of methyl groups for molecules outside of an aggregate structure. Since there are both small clusters and large aggregates in the sample, the quenched phosphorescence data were fit to the sum of two first-order decays to account for excited benzophenone encountering these two methylated colloid structures:

$$I(t) = A \exp\left(\frac{-t}{\tau_1}\right) + B \exp\left(\frac{-t}{\tau_2}\right) \qquad (3)$$

where A and B are the relative phosphorescence intensities from the two populations, while τ_1 and τ_2 represent their lifetimes.

A Stern−Volmer analysis was used to determine the rate constant of quenching by methyl groups in these two populations of aggregates. The observed decay rates ($k_{obs} = 1/\tau$) are plotted versus the total concentration of methyl groups (solid circles) in Figure 4. Note that both Stern−Volmer plots converge on the same intercept, which indicates that the dispersion in decay rates is related *only* to quenching by the colloids. The apparent quenching rate constant for the dispersed, small clusters was determined from the slope in Figure 4a to be $k_1 = (1.4 \pm 0.1) \times 10^6\ M^{-1}\ s^{-1}$. A locally higher concentration of methyl groups is present within aggregates and produces a faster H-atom abstraction rate constant, as found from the slope in Figure 4b, $k_2 = (9.0 \pm 1.1) \times 10^6\ M^{-1}\ s^{-1}$. The experiment was repeated and was reproducible within the error of fitting the decay transients. The weighted averaged rate constants from both trials are $k_1 = (1.6 \pm 0.1) \times 10^6\ M^{-1}\ s^{-1}$ for the small clusters and $k_2 = (9.9 \pm 1.0) \times 10^6\ M^{-1}\ s^{-1}$ for the large aggregates.

These rate constants are based on the *total* concentration of methyl groups in the sample; the actual rate constants for the quenching reaction should account for the fractional concentration of methyl groups in the two populations of colloids. The initial intensity of phosphorescence decay transient (preexponential factor) depends on the product of the phosphorescence emission rate constant and the population of excited states. If the emission rate constant from the two populations of benzophenone is not affected by the quenching environment, then the amplitudes of the phosphorescence decays (A and B from eq 3) will be proportional to the populations of excited triplets undergoing quenching by the two types of colloids. Figure 5 is a plot of the amplitudes of the two phosphorescence decay components versus total methyl-group concentration on the lower x-axis and total colloid concentration on the upper x-axis. The fraction of triplets quenched by small clusters decreases as the colloid concentration (and aggregation) increases, while the fraction of triplets quenched by highly aggregated sites increases with colloid concentration, as expected. At the lowest colloid concentration, 2.7 mg/mL, approximately 88% of the excited states are quenched by small clusters; however, at the highest concentration, 15.1 mg/mL, the fraction of excited states quenched by small clusters decreases to 69%, with the remainder of quenching being effected by large aggregates.

To determine the quenching rate constants for the two types of colloid in the sample, the methyl-group concentrations are apportioned between the populations of particles of each type. The fraction of dispersed and aggregated colloids are estimated from the relative amplitudes of phosporescence emission from the two decaying populations of benzophenone, which assumes that benzophenone is homogeneously dispersed within the two colloid populations. The open circles in Figure 4 represent measured decay rates plotted at methyl-group concentrations that have been adjusted for the fractional populations of dispersed and aggregated colloids, and the dashed lines are linear least-squares fits to the data. The corrected rate constant for triplet quenching from methyl groups on small, colloid clusters was determined from the average of two trials to be $k_{1,adj} = (2.2 \pm 0.1) \times 10^6\ M^{-1}\ s^{-1}$, while the quenching rate by methyl groups in large, aggregates was found to be $k_{2,adj} = (5.4 \pm 0.5) \times 10^7\ M^{-1}\ s^{-1}$. The quenching by methyl groups in the aggregated sites is much faster due to the locally higher quencher concentration experienced by triplet states within these structures.

The quenching rate for both populations appears to be slower at the highest colloid concentrations, which is evident in a deviation from linearity in the corrected Stern−Volmer plots. While adding a nonlinear term to fitting these data does not produce a significant improvement in the quality of fit due to the uncertainty in the measured decay rates, the systematic deviation of the decay rates from a Stern−Volmer relationship at higher concentrations may be real. This behavior could indicate a saturation effect that would be expected if adsorption of the triplet probe to the colloid surface captures a significant fraction of the excited population at high concentrations and dominates the quenching process (see below).

Comparison to Free-Solution Quenching Kinetics. The rate constants for interfacial quenching of benzophenone triplet states by silica-bound methyl groups were compared to the rates of quenching by two homogeneous solution model compounds: methanol and hexamethyldisiloxane or HMDS, $((CH_3)_3Si)_2O$. The rate of quenching by H-atom abstraction is sensitive to the C−H bond strength of the H-atom donor,[39,41,46] which is 94 kcal/mol for methanol[47] and 99 kcal/mol for HMDS (calculated

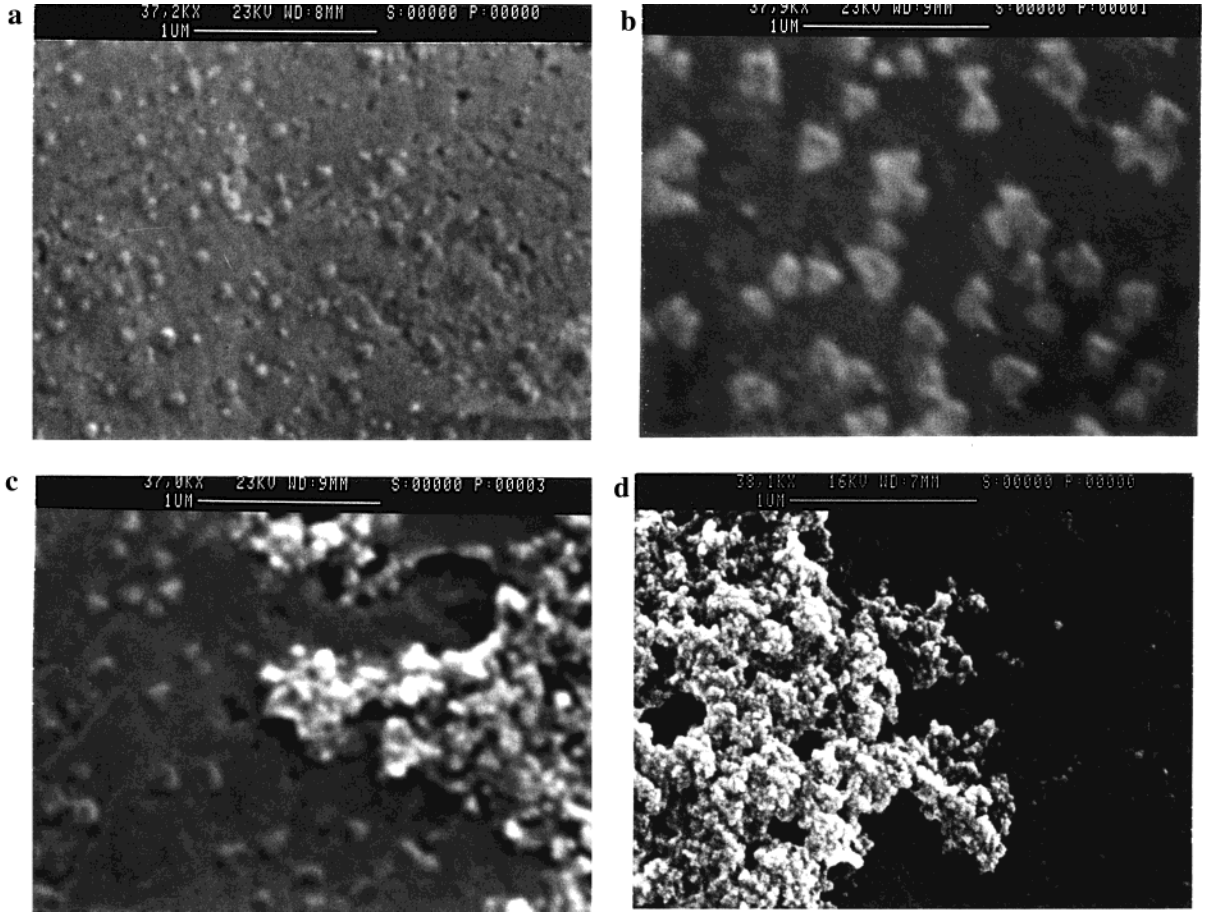

Figure 3. SEM images of the methylated colloids: (a) 2.7 mg/mL colloids; (b) 6.3 mg/mL colloids; (c) 10.7 mg/mL colloids; (d) 15.1 mg/mL colloids.

from the heat of formation[48]). The C−H bond strengths of these solution model compounds are similar, which should lead to comparable intrinsic rates of quenching by H-atom transfer. Benzophenone phosphorescence was quenched by methanol over concentrations ranging from 0 to 35 mM, and a Stern−Volmer plot of the results is shown in Figure 6, where the rate constant for quenching is determined to be $k_{q,MeOH} = (2.1 \pm 0.2) \times 10^5\ M^{-1}\ s^{-1}$. Benzophenone phosphorescence was also quenched by hexamethyldisiloxane at concentrations varied from 0 to 30 mM (see Figure 7); the rate constant for quenching, based on the total methyl-group concentration, was determined as one-sixth of the slope of the plot, $k_{q,HMDS} = (5.8 \pm 0.1) \times 10^4\ M^{-1}\ s^{-1}$.

Immobilizing the quencher at a surface reduces access from solution and lowers the rate of collisional encounter in the absence of adsorption.[49] This effect can be observed in the smaller quenching rate by methyl groups bound to hexamethyldisiloxane compared to methanol, since methyl groups bound to the larger molecule are not free to diffuse but must diffuse at the slower rate of a larger species in solution. Rates of reaction at an interface, with one reactant immobilized at a spherical surface, can be derived[49,50] starting from the Smoluchowski euation[51] for predicting rate constants of solution-phase reactions:

$$k_{q,Q} = \frac{4\pi N_{AV} R_{Q+BP} D_{Q+BP}}{1000} \exp(-E_{a,Q}/kT) \qquad (4)$$

where N_{AV} is Avogadro's number, R_{Q+BP} is the sum of radii of benzophenone and the quencher, and D_{Q+BP} is the mutual diffusion coefficient given by the sum of $D_Q + D_{BP}$. The time-dependent term of the Smoluchowski equation is negligible at long times ($t \gg R^2/D \approx 0.5$ ns). Since the reaction is not diffusion-controlled, an Arrhenius factor, $\exp(-E_{a,Q}/kT)$, corrects for the fraction of collisions that do not result in reaction.

In the heterogeneous quenching experiments, the quencher is immobilized at the surface of a colloid and reacts with triplet benzophenone diffusing in solution. While the large aggregates cannot be modeled by a simple structure, the more dispersed, small clusters of colloids can be represented as hard spheres having an average radius, R_P. The radius of this sphere is much greater than the size of benzophenone so that the encounter radius, R_{P+BP}, is dominated by the radius of the sphere, R_P; similarly, diffusion of the particle is much slower than benzophenone so that most of the mutual diffusion coefficient, D_{P+BP}, is due to the motion of benzophenone, D_{BP}. The rate of quenching of triplet benzophenone by methyl groups bound to the surface of silica particles will be described by

$$k_{q,P} = \frac{4\pi N_{AV} R_{P+BP} D_{P+BP}}{1000 n_{P/Q}} \exp(-E_{a,P}/kT) \qquad (5)$$

where $n_{P/Q}$ is the number of methyl groups on each particle and $E_{a,P}$ is the activation energy for the quenching reaction at the particle surface.

The ratio of rate constants for particle-bound methyl groups ($k_{q,P}$) versus free-solution ($k_{q,Q}$) quenching represents the kinetic effect of immobilizing the methyl groups on a surface:

$$\frac{k_{q,P}}{k_{q,Q}} = \frac{R_{P+BP} D_{P+BP}}{R_{Q+BP} D_{Q+BP} n_{P/Q}} \exp(-\Delta E_a/kT) \qquad (6)$$

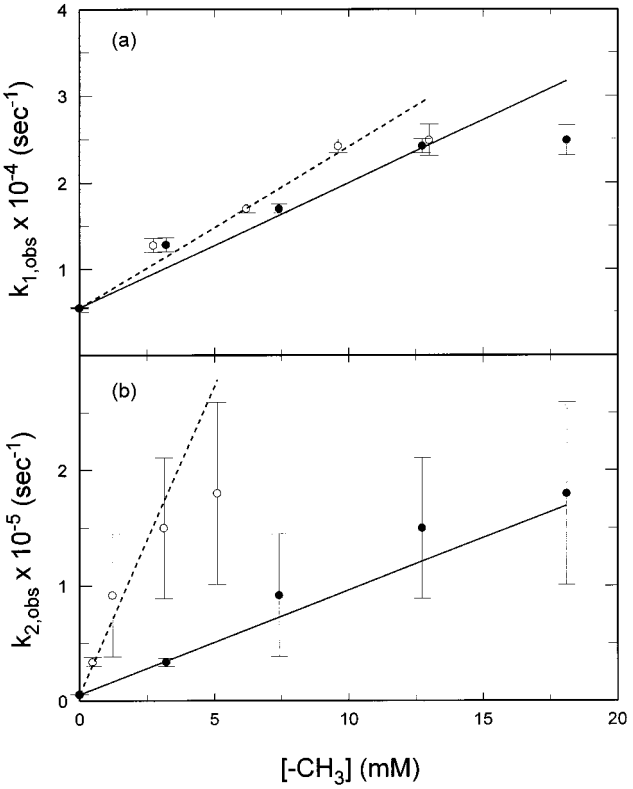

Figure 4. Stern−Volmer plot of the observed benzophenone phosphorescence decay rate versus methyl-group concentration. (a) Quenching rate for small clusters of colloids: solid circles, total methyl-group concentration; open circles, corrected methyl-group concentration. The quenching rate constant from the small colloid clusters is determined from the slope to be $k_1 = (2.2 \pm 0.1) \times 10^6$ M^{-1} s^{-1}. (b) Quenching rate for aggregated colloids: solid circles, total methyl-group concentration; open circles, corrected methyl-group concentration. The quenching rate constant from the aggregated colloids is determined from the slope to be $k_2 = (5.4 \pm 1.5) \times 10^7$ M^{-1} s^{-1}.

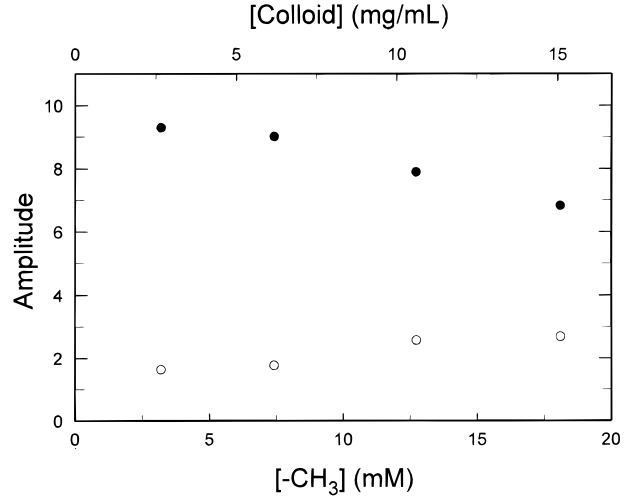

Figure 5. Phosphorescence amplitudes (proportional to the triplet populations) versus total methyl-group concentration on the lower *x*-axis and colloid concentration on the upper *x*-axis. Solid circles are phosporescence amplitudes for excited states quenched by small clusters and open circles are amplitudes for quenching by large aggregates.

This expression is first used to evaluate the relative quenching rates of hexamethyldisiloxane compared to methanol. The radii of benzophenone, methanol, and HMDS were determined from energy-minimized geometries from HyperChem to be 0.38, 0.14, and 0.32 nm, respectively; these values were used to estimate the ratio: $R_{P+BP}/R_{Q+BP} \approx 1.35$, which is greater than 1 due to

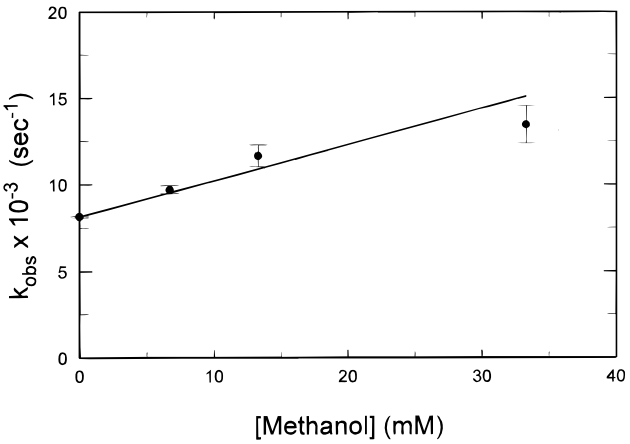

Figure 6. Stern−Volmer plot of the benzophenone phosphorescence decay rate, k_{obs}, versus methanol concentration in 50/50 acetonitrile/water. The homogeneous free-solution H-atom abstraction rate constant by methanol is determined from the slope to be $(2.1 \pm 0.2) \times 10^5$ M^{-1} s^{-1}.

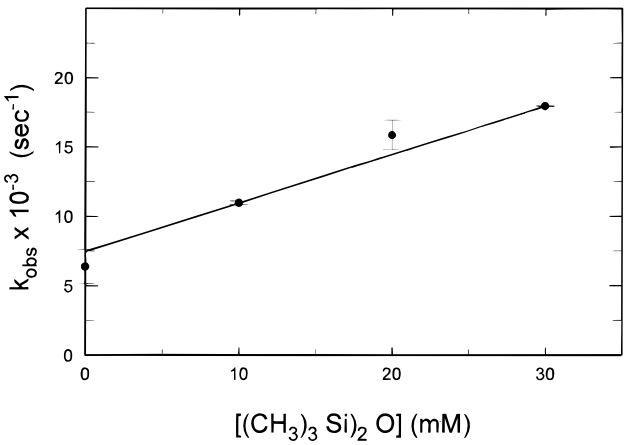

Figure 7. Stern−Volmer plot of the benzophenone phosphorescence decay rate, k_{obs}, versus hexamethyldisiloxane concentration in 50/50 acetonitrile/water. The slope of the plot is $(3.5 \pm 0.1) \times 10^5$ M^{-1} s^{-1}. The homogeneous free-solution H-atom abstraction rate constant by methyl groups in hexamethyldisiloxane is calculated from $^1/_6$ slope and found to be $(5.8 \pm 0.1) \times 10^4$ M^{-1} s^{-1}.

the larger size of HMDS compared to methanol. The ratio of mutual diffusion coefficients is estimated using the Stokes−Einstein relation, $D = kT/6\pi R\eta$, where R is the radius and η is the solution viscosity. Using this relation, the ratio of mutual diffusion coefficients is predicted from the radii of the diffusing species:

$$\frac{D_{P+BP}}{D_{Q+BP}} = \frac{1/R_P + 1/R_{BP}}{1/R_Q + 1/R_{BP}} \tag{7}$$

which is 0.59 for HMDS compared to methanol, due the slower diffusion rate of the larger quencher molecule.

Using the ratio of radii and diffusion coefficients along with the number of methyl groups per HMDS molecule, $n_{P/Q} = 6$, eq 6 predicts a reduction in the rate constant for benzophenone triplet quenching by a factor $k_{q,P}/k_{q,Q} = 0.13$ based solely on changes in the collision frequency (neglecting changes in activation energy for the reaction). The observed reduction in the rate of quenching by methyl groups in HMDS compared to quenching by methanol was 0.28 (±0.3), which is not quite as large as predicted by eq 6, neglecting changes in the activation energy. Despite the 5% larger C−H bond dissociation energy

for HMDS, the quenching efficiency of siloxane-bound methyl groups appears to be about 2-fold larger than methanol. Since methyl groups are bound to the colloidal silica particles through siloxane linkages, HMDS is a better solution-phase model compound to use for analyzing kinetics of interfacial quenching by the methylated silica.

To understand the reduction in collisional encounters between triplet benzophenone and methyl groups bound to the silica particles, the quenching kinetics for the dispersed colloid clusters were compared to quenching by HMDS. The radius of the small clusters (determined from the SEM image to be $R_P \approx 10.5$ nm) and the radii of benzophenone and HMDS were used to estimate the ratio, $R_{P+BP}/R_{Q+BP} \approx 15.0$, where the free-solution model, Q, now refers to HMDS. Because of the large size of the silica particles, the mutual diffusion coefficient for quenching interfacial quenching is dominated by the diffusion of benzophenone, $D_{P+BP} \approx D_{BP}$, which allows the ratio with the HMDS value to be simplified: $D_{P+BP}/D_{Q+PB} = R_Q/(R_{BP} + R_Q) = 0.46$.

The ratio of quencher groups on the colloid clusters compared to the free-solution model, $n_{P/Q}$, is estimated from the number of methyl groups per gram of silica. The spherical volume of an individual silica colloid particle (radius = 3.5 nm) and the density of fused silica ($\rho = 2.2$ g/cm^3) determine the mass of a single particle (3.95×10^{-19} g/particle). The number of methyl groups per colloid was then calculated from the measured specific surface area and methyl-group surface coverage to be 285 $-CH_3$ groups per particle. In a hexagonally close-packed arrangement, 13 colloids may be packed into the cluster having a radius of 10.5 nm that matches the radius measured in the SEM images. Since the methylation of the silica occurs in a gas-phase reaction prior to aggregation, the methyl groups should be dispersed over the entire particle surface. In a closed-packed cluster, about half of the surface area of each colloid particle would be accessible for reaction from solution. Therefore, the ratio of available quenching sites for the cluster compared to HMDS is $n_{P/Q} \approx (285 \times 13/2)/6 = 308$. The final factor that affects $k_{q,P}/k_{q,Q}$ is any difference in the energy barrier for reaction, $\exp(-\Delta E_a/kT)$; this term is likely to be small since the solution-phase model compound carries the same methyl-group chemistry as the methylated silica. If this term is neglected, then the predicted reduction in the quenching rate by silica-bound methyl groups is $k_{q,P}/k_{q,Q} = 0.022$. This factor indicates that, based on a reduction in collision frequency, quenching by methyl groups on the silica should occur at a much slower rate than quenching by HMDS.

Despite the predicted reduction in collision frequency due to immobilization of the quencher on the colloid, the observed rate constant for quenching of triplet benzophenone by silica-bound methyl groups was found to be 38 times *larger* than by methyl groups on HMDS, $k_{1,adj} = (2.2 \pm 0.1) \times 10^6$ M^{-1} s^{-1} versus $k_{q,HMDS} = (5.8 \pm 0.1) \times 10^4$ M^{-1} s^{-1} (see above). A rate enhancement of a heterogeneous reaction can be observed if the surface plays a significant role in the frequency of encounters between reacting molecules. Interfacial reactions can occur through a direct (Eley-Rideal) and/or indirect (Langmuir−Hinshelwood) mechanism.[52] Up to this point, a direct mechanism with diffusional encounter from solution has been assumed. The indirect mechanism proceeds through adsorption of one reactant followed by surface diffusion to a reactive site, which can result in significant rate enhancements in comparison to an analogous reaction in free solution.[49,50,53] In the present results, quenching at the colloid/solution interface is about 3 orders of magnitude faster than the rate expected from the free-solution rate corrected for the reduction in direct collision frequency from solution. This suggests that an indirect mechanism is likely responsible for the enhancement of the reaction rate compared with free solution. While the fraction of adsorbed benzophenone is small (≤2%, see above), nevertheless, the potential residence time on the surface ($t_{res} \leq 600$ ns) is sufficient to greatly increase the probability of interfacial quenching compared to collisional encounters in solution. The upper bound to surface residence is more than 4 orders of magnitude greater than a typical encounter time in a solvent cage in free solution;[54] the time that the quencher can reside at the interface can, therefore, easily account for a 3 order-of-magnitude enhancement in the rate of quenching.

Detection of Diphenylketyl Radicals. To verify that quenching of triplet benzophenone by methylated silica proceeds by H-atom abstraction from surface methyl groups, the generation of benzophenone ketyl radicals in the sample upon photolysis was tested in a laser-induced fluorescence experiment. Diphenylketyl radicals were excited to their excited doublet state using a continuous wave (cw) laser at 514.5 nm, and fluorescence emission from the doublet excited state[55] was detected in the region of 550−650 nm.[33] The radical population decays primarily by homolytic recombination[33,37] with a rate given by

$$\frac{d[Ph_2\dot{C}OH]}{dt} = -2k_r[Ph_2\dot{C}OH]^2 \qquad (8)$$

Separation of variables and integration over time yields a simple second-order decay represented by

$$I(t) = \frac{A_f}{1 + \alpha t} \qquad (9)$$

where A_f is the initial radical fluorescence intensity (which depends on the initial radical concentration, $[Ph_2\dot{C}OH]_0$) and where the initial second-order rate is $\alpha = 2k_r[Ph_2\dot{C}OH]_0$. The initial radical concentration was varied by controlling the excitation laser energy to vary the concentration of excited-triplet states, $[Ph_2\dot{C}OH]_0 = [^3Ph_2CO]k_q[Q]/(k_o + k_q[Q])$. These experiments were carried out at the lowest colloid concentration, 2.7 mg/mL, to avoid a significant fraction of large aggregates and signal loss due to scattering. The 355 nm excitation laser pulse energies used were 250, 420, 650, and 890 μJ/pulse corresponding to initial ketyl radical concentrations of 0.19, 0.32, 0.50, and 0.69 μM, accounting for the fractional concentrations and the corresponding quenching rate constants from the two colloidal environments and assuming that each quenching event leads to a free ketyl radical in solution. Radical fluorescence transients along with best fits to a second-order decay model are plotted in Figure 8. Figure 9 shows a Stern−Volmer analysis of the initial second-order rates, α, versus the initial ketyl radical concentration, the slope of which is twice the apparent recombination rate constant, $k_{r,app} = (2.7 \pm 0.8) \times 10^7$ M^{-1} s^{-1}, in the presence of colloids.

To determine whether the colloid particles influence either the radical generation or recombination process, the free-solution ketyl radical recombination rate constant was determined by the photoreduction of triplet benzophenone by benzhydrol (BPH_2) in 50/50 ACN/H_2O at pH = 6.3 in the absence of colloids. Two diphenylketyl radicals are produced by this quenching process:

$$^3Ph_2CO + Ph_2CHOH \rightarrow 2[Ph_2\dot{C}OH]_0 \qquad (10)$$

The quantum yield for ketyl radical production is given by $\phi_k = 2k_q[BPH_2]/(k_0 + k_q[BPH_2])$, where k_q is the quenching rate

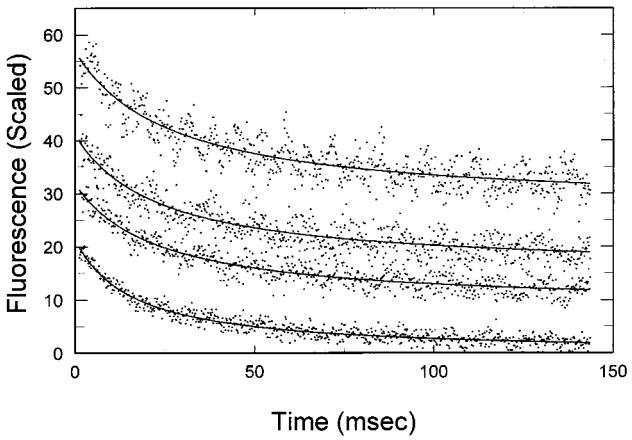

Figure 8. Diphenylketyl radical fluorescence transients. Triplet benzophenone is quenched by methylated colloids at a methyl-group concentration of 3.2 mM in 50/50 ACN/H_2O at pH = 6.2. The 355 nm excitation laser pulse energy was varied from top to bottom as follows: 250, 420, 650, and 890 μJ. The transients are scaled to the same amplitude, offset for viewing, and fit to a second-order decay model, eq 9.

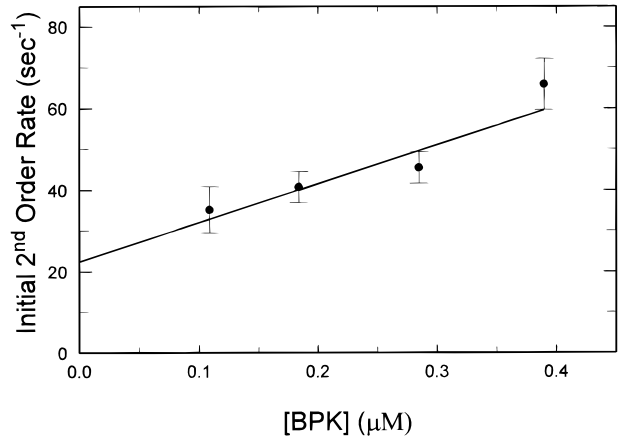

Figure 9. Second-order radical recombination rate versus the initial ketyl radical concentration. The radical concentrations were varied by changing the excitation fluence at a fixed probe power of 500 mW. The apparent ketyl radical recombination rate constant in the presence of colloids was determined from $^1/_2$ slope to be $k_r = (2.7 \pm 0.8) \times 10^7$ M^{-1} s^{-1}.

constant and k_0 is the unimolecular decay rate. With the unimolecular decay rate $k_0 = 7900$ s^{-1} and a quencher concentration [BPH_2] = 3 mM, the quantum yield of ketyl radical production was $\phi_K = 1.64$. Figure 10 shows example ketyl radical decay transients along with best fits to a second-order decay model of eq 9. Laser pulse energies of 170, 290, 400, and 480 μJ/pulse correspond to ketyl radical concentrations of 0.25, 0.43, 0.59, and 0.71 μM. A Stern−Volmer analysis was used to determine the free-solution recombination rate constant, $k_r = (9.0 \pm 0.8) \times 10^7$ M^{-1} s^{-1}, in 50/50 ACN/H_2O in the absence of colloids, as plotted in Figure 11. The ketyl radical recombination rate constant in 50/50 ACN/H_2O is 2.1 times slower than the rate constant for recombination in pure acetonitrile;[33] the higher viscosity of a 50/50 ACN/H_2O solution ($\eta = 0.87$ cP versus 0.34 cP for pure acetonitrile) would predict a 2.6-fold lower rate in the mixed solvent, which is comparable to the observed results.

The apparent ketyl radical recombination rate constant in the presence of colloids is one-third of the rate constant observed for diphenylketyl recombination in free solution. Some of this difference could be due to colloidal aggregates slowing the rate

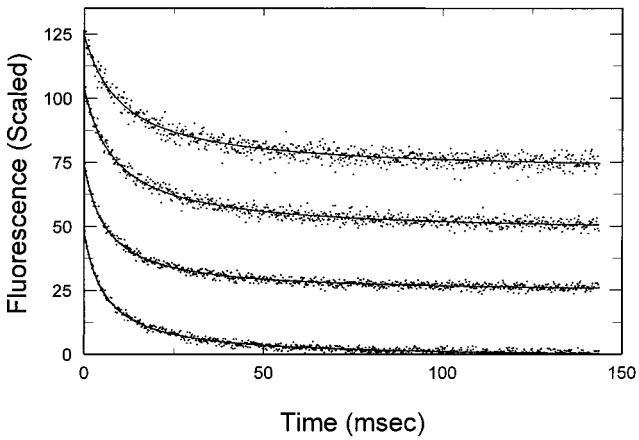

Figure 10. Free-solution benzophenone ketyl radical decay transients. Triplet benzophenone was quenched by free-solution 3 mM benzhydrol in 50/50 ACN/H_2O at pH = 6.3. The 355 nm excitation laser pulse energy was varied from top to bottom as follows: 170, 290, 400, and 480 μJ. The transients are scaled to the same amplitude, offset for viewing, and fit to a second-order decay model, eq 9.

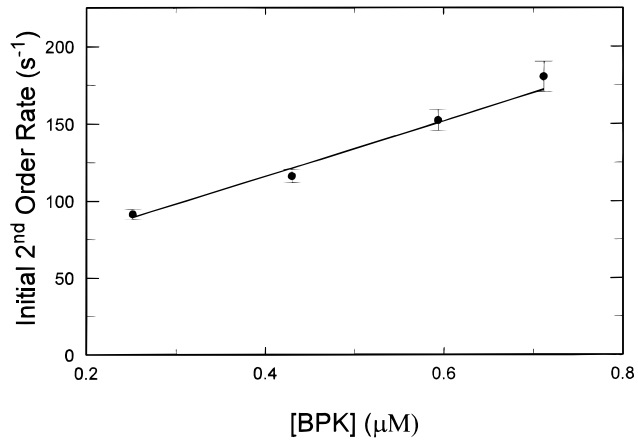

Figure 11. Initial second-order radical recombination rate in free solution versus ketyl radical concentration. The radical concentrations were varied by changing the excitation fluence at a fixed probe power of 500 mW. The free-solution ketyl radical recombination rate constant was determined from $^1/_2$ slope to be $k_r = (9.0 \pm 0.8) \times 10^7$ M^{-1} s^{-1}.

of diffusive encounter between radicals; inhibition of diffusive encounters between molecules even within the pores of precipitated silica, however, is much smaller than this factor for diffusion over distances up to 0.7 μm.[56] The slower apparent recombination rate constant in the presence of colloids more likely arises from a significant decrease in the *yield* of free radicals in solution. The number of free radicals that escape the surface and diffuse into solution can be less than the initial number of ketyl radicals produced by quenching due to an efficient heterolytic coupling reaction between the ketyl radical and the immobilized methyl radical. Adsorption of the ketyl radical to the colloid surface could greatly enhance this rate compared to a free-solution process. Desorption of the ketyl radical from the colloid surface into solution would compete with radical coupling to the silica-immobilized methyl radical. Surface-coupling of Norrish-Type II generated radicals has previously been employed for surface modification of polymers using benzophenone precursors in solution.[8,57] These surface photoreactions should also proceed by this mechanism.

Summary

Dispersed colloids possess many advantages over flat surfaces and porous particles as model surfaces for the investigation of

interfacial kinetics. The kinetics of the H-atom abstraction from methyl groups immobilized at the fumed silica surface by triplet benzophenone was monitored by phosphorescence quenching, and the intermediate diphenylketyl radicals were detected using a time-resolved fluorescence technique. The results indicate colloidal aggregation plays a role in the quenching of the triplet state leading to a dispersion in reaction rates. The amplitudes of the fitted data were used to correct the rate constants for the actual fraction of methyl groups present as clusters and as aggregates. The rate constant for quenching by aggregated colloids was found to be 20 times greater than quenching by small dispersed clusters, due to the higher local concentration of methyl groups within an aggregate. Because of the spherical shape of the small clusters, the rate constant for quenching of triplet benzophenone by these particles could be compared theoretically with quenching by a free-solution model compound, hexamethyldisiloxane. A significant enhancement of the reaction rate at the colloid particle surface is believed to arise from an indirect (Langmuir−Hinshelwood) mechanism, where adsorption of the excited-triplet precursor greatly increases the yield of the quenching reaction.

The ketyl radical intermediate from the H-atom transfer from methylated colloids was detected by cw laser-induced fluorescence. An apparent recombination rate constant was determined from the decay of fluorescence from free radicals to be slower by a factor of one-third in the presence of colloids compared to a free-solution rate. The discrepancy most likely arises from adsorption of the intermediate ketyl radical and a heterolytic coupling reaction with the alkyl radical immobilized on the colloid surface, which lowers the yield of free radicals that diffuse in solution.

Acknowledgment. This research was supported in part by the National Science Foundation under Grant CHE98-17534. R976 methylated colloids were donated by the Degussa Corp., Dublin, OH. The authors acknowledge the assistance of Denise Chirban, who acquired the SEM images, and Dion Rivera, who measured the infrared spectrum of the methylated silica.

References and Notes

(1) *Environmental Photochemistry*; Boule, P., Ed.; Springer: Berlin, 1999.

(2) Kamat, P. V. *Chem. Rev.* **1993**, *93*, 267−300.

(3) Nosaka, Y.; Kishimoto, M.; Nishino, J. *J. Phys. Chem. B* **1998**, *102*, 79−83.

(4) Dressick, W. J.; Calvert, J. M. *Jpn. J. Appl. Phys.* **1993**, *32*, 5829−5839.

(5) Ledwith, A. In *Photochemistry and Polymeric Systems*; Kelly, J. M., McArdle, C. B., de F. Maunder, M. J., Eds.; Royal Society of Chemistry: London, 1993; pp 1−14.

(6) Huang, J.; Dahlgren, D. A.; Hemminger, J. C. *Langmuir* **1994**, *10*, 626−628.

(7) Roffey, C. *Photogeneration of Reactive Species for UV Curing*; John Wiley and Sons: Chichester, U.K., 1997; Chapter 1.

(8) Swanson, M. J.; Dunkirk, S. G.; Pietig, J. A.; Guire, P. E. *Chemtech* **1992**, *22*, 624−626.

(9) Dorman, G.; Prestwich, G. D. *Biochemistry* **1994**, *33*, 5661−5673.

(10) Dunkirk, S. G.; Gregg, S. L.; Duran, L. W.; Monfils, J. D.; Haapala, J. E.; Marcy, J. A.; Clapper, D. L.; Amos, R. A.; Guire, P. E. *J. Biomater. Appl.* **1991**, *6*, 131−156.

(11) de Mayo, P. *Pure Appl. Chem.* **1982**, *54*, 1623−1632.

(12) Oelkrug, D.; Flemming, W.; Füllemann, R.; Günther, R.; Honnen, W.; Krabichler, G.; Schäfer, M.; Uhl, S. *Pure Appl. Chem.* **1986**, *58*, 1207−1218.

(13) Thomas, J. K. *J. Phys. Chem.* **1987**, *91*, 267−276.

(14) Turro, N. J. *Tetrahedron* **1987**, *43*, 1589−1616.

(15) Thomas, J. K. *Chem. Rev.* **1993**, *93*, 301−320.

(16) Krasnansky, R.; Thomas, J. K. *J. Photochem. Photobiol. A: Chem.* **1991**, *57*, 81−96.

(17) Samuel, J.; Ottolenghi, M.; Avnir, D. *J. Phys. Chem.* **1991**, *95*, 1890−1895.

(18) Wong, A. L.; Harris, J. M. *J. Phys. Chem.* **1991**, *95*, 5895−5901.

(19) Kavanagh, R. J.; Thomas, J. K. *Langmuir* **1998**, *14*, 352−362.

(20) Levin, P. P.; Costa, S. M. B.; Ferreira, L. F. V. *J. Phys. Chem.* **1996**, *100*, 15171−15179.

(21) Unger, K. K. *Porous Silica*; Elsevier Scientific: New York, 1979; Appendix A.

(22) Wong, A. L.; Hunnicutt, M. L. Harris, J. M. *J. Phys. Chem.* **1991**, *95*, 4489−4495.

(23) McKay, G.; Otterburn, M. S.; Aga, J. A. *J. Chem. Technol. Biotechnol.* **1987**, *34*, 247−256.

(24) Drake, J. M.; Klafter, J.; Levitz, P. In *Dynamical Processes in Condensed Molecular Systems*; Klafter, J., Jortner, J., Blumen, A., Eds.; World Scientific: Singapore, 1989; pp 246−267.

(25) Hallmann, M.; Unger, K. K.; Appel, M.; Fleischer, G.; Kärger, J. *J. Phys. Chem.* **1996**, *100*, 7729−7734.

(26) Avnir, D.; Farin, D.; Pfeifer, P. *J. Chem. Phys.* **1983**, *79*, 3566−3571.

(27) Wellner, E.; Ottolenghi, M.; Avnir, D. *Langmuir* **1986**, *2*, 616−619.

(28) Carraway, E. R.; Demas, J. N.; DeGraff, B. A. *Langmuir* **1991**, *7*, 2991−2998.

(29) Osipov, V. V.; Samoilenko, Y. Y.; Ritter, A. Y.; Shkilev, V. P.; Bogillo, V. I. *Chem. Phys. Rep.* **1997**, *16*, 1247−1262.

(30) Bogillo, V. I.; Shkilev, V. P.; Osipov, V. V. *Langmuir* **1997**, *13*, 945−950.

(31) Wong, A. L.; Harris, J. M.; Marshall, D. B. *Can. J. Phys.* **1990**, *68*, 1027−1034.

(32) Forbes, M. D. E.; Ruberu, S. R.; Dukes, K. E. *J. Am. Chem. Soc.* **1994**, *116*, 7299−7307.

(33) Shield, S. R.; Harris, J. M. *Anal. Chem.* **1998**, *70*, 2576−2583.

(34) Technical Bulletin Pigments, No. 6; Degussa Corp., Germany, 1990.

(35) Bates, R. G.; Paabo, M.; Robinson, R. A. *J. Phys. Chem.* **1963**, *67*, 1833−1838.

(36) Jensen, R. P.; Eyring, E. M.; Walsh, W. M. *J. Phys. Chem.* **1966**, *70*, 2264−2270.

(37) Pitts, J. N.; Letsinger, R. L.; Taylor, R. P.; Patterson, J. M.; Recktenwald, G.; Martin, R. B. *J. Am. Chem. Soc.* **1959**, *81*, 1068−1077.

(38) Moore, W. M.; Hammond, G. S.; Foss, R. P. *J. Am. Chem. Soc.* **1961**, *83*, 2789−2794.

(39) Beckett, A.; Porter, G. *Trans. Faraday Soc.* **1963**, *59*, 2038−2050.

(40) Hammond, G. S.; Turro, N. *Science* **1963**, *142*, 1541−1543.

(41) Walling, C.; Gibian, M. J. *J. Am. Chem. Soc.* **1965**, *87*, 3361−3364.

(42) Weiner, S. A. *J. Am. Chem. Soc.* **1971**, *93*, 425−429.

(43) Cohen, S. G.; Parola, A.; Parsons, G. H. *Chem. Rev.* **1973**, *73*, 141−161.

(44) Simon, J. D.; Peters, K. S. *Chem. Rev.* **1984**, *17*, 277−283.

(45) Ren, F. Y.; Waite, S. W.; Harris, J. M. *Anal. Chem.* **1995**, *67*, 3441−3447.

(46) Ledger, M. B.; Porter, G. *J. Chem. Soc., Faraday Trans. I* **1972**, *68*, 539−46.

(47) *CRC Handbook of Chemistry and Physics*, 71st ed.; Lide, D. R., Ed.; CRC Press: Boston, 1990.

(48) Wagman, D. D.; Evan, W. H.; Halow, I.; Parker, V. B.; Bailey, S. M.; Schumm, R. H. *Selected Values for of Chemical Thermodynamic Properties: Part 2; Tables for the Elements Twenty-Tree through Thirty-Two in Standard Order of Arrangement*; Technical Note 270-2; National Bureau of Standards: Washington, DC, 1966; Table 24(6).

(49) Astumian, R. D.; Schelly, Z. A. *J. Am. Chem. Soc.* **1984**, *106*, 304−308.

(50) Astumian, R. D.; Chock, P. B. *J. Phys. Chem.* **1985**, *89*, 3477−3482.

(51) Smoluchowski, M. V. *Z. Phys. Chem.* **1917**, *92*, 129−168.

(52) Atkins, P. W. *Physical Chemistry*, 4th ed.; WH Freeman: New York, 1978; pp 895−896.

(53) Wang, D.; Gou, S.-Y.; Alexrod, D. *Biophys. Chem.* **1992**, *43*, 117−137.

(54) Miers, J. B.; Postlewaite, J. C.; Zhuang, T.; Chen, S.; Romemig, R.; Wen, X.; Dlott, D. *J. Chem. Phys.* **1990**, *93*, 8771−8776.

(55) Razi Naqvi, K.; Wild, U. P. *Chem. Phys. Lett.* **1976**, *41*, 570−574.

(56) Shield, S. R. Ph.D. Dissertation, University of Utah, 1999; manuscript in preparation.

(57) Allen, N. S. *J. Photochem. Photobiol. A: Chem.* **1996**, *100*, 101−107.